29th Congress of the International Council of the Aeronautical Sciences
St. Petersburg, Russia; September 7-12, 2014

NUMERICAL INVESTIGATION OF LAMINAR NEAR WAKE SEPARATION ON CIRCULAR CYLINDERS AT SUPERSONIC VELOCITIES

W. Schuyler Hinman*, Craig T. Johansen*, Chris J. Arisman*, Wagner C. Galuppo*
***Department of Mechanical Engineering, University of Calgary**

Abstract

Laminar separation on the aft-body of an adiabatic circular cylinder was numerically investigated over a range of freestream Mach ($2<Ma<10$) and Reynolds ($10^3<Re<10^5$) numbers. Simulation predictions are compared to various experimental results and to theories presented over the last 60 years. The often used hypersonic Mach number independence assumption is challenged by the present results, which show a highly interdependent relationship between Mach number and Reynolds number, even at high Mach numbers in the present case. A theory explaining this relationship, which is based on interactions between the inviscid outer-flow and the viscous boundary layer flow near the separation point, is proposed. Connections to similar flows such as converging-diverging nozzles, compression corners, and shockwave boundary layer interactions are discussed. An estimation of the uncertainty associated with using surface pressure measurements to identify the separation location, which is commonly done in other experiments, is also given.

1 Introduction

The prediction of flow separation and the near-wake structure behind blunt bodies at hypersonic speeds has been largely motivated by the development of atmospheric entry vehicles and the ballistic missile program in the 60's [1]. The near-wake structure can have a large impact on the vehicle heating loads, dictating the aft-body heat-shield design requirements [2]. In a work by Schneider, surface roughness on an entry capsule fore-body was found to completely suppress large-scale flow separation in the wake, which increased the heating loads on the aft-body [3]. More recently, the near-wake of the Mars Science Laboratory (MSL) aero-shell was analyzed to study potential aerodynamic interference problems associated with the Reaction Control System (RCS) jets [4]. The RCS jets were used to actively dampen aerodynamic perturbations and to perform bank-reversal maneuvers in order to improve the landing accuracy and reduce vehicle momentum at high altitudes. Early RCS jet designs showed poor control authority as a result of these unwanted aerodynamic interactions [5]. As a result, interactions between the RCS jets and the near-wake and between individual RCS jets were studied both experimentally and numerically [4-6]. During that work, it was found that the shape of the three-dimensional wake behind the MSL aero-shell could be predicted qualitatively using a Reynolds number dependent empirical correlation based on post-shock Reynolds number that was presented by Park *et al.* [7].

Although there is abundant literature on hypersonic flows around blunt bodies, work has mainly focused on predicting fore-body aerodynamic loads related to heat-shield design or predicting magnitudes of base pressure on the aft-body. The majority of previous work on the near-wake has mainly focused on flow behind slender bodies such as cones and wedges [8-10], and bluff bodies such as bullets and circular cylinders [11-17]. The primary difference between a cone-type body and a circular cylinder is that separation occurs suddenly at a fixed location coinciding with the sharp trailing edge of the cone, while on a circular cylinder the separation location is determined by the presence of an adverse pressure gradient [8]. Understanding the effects of Mach and

Reynolds numbers on these shapes is the primary motivation of this work.

In the past both Mach number and Reynolds number were considered to be only mildly important to parameters such as body pressure distribution [18]. It is now well known that the near-wake structure behind hypersonic blunt bodies is heavily dependent on Reynolds number [8,11-16]. In contrast, less work has been reported on the combined effect of Mach number and Reynolds number on the near-wake structure. At high Mach numbers, it is often still argued that the wake flow is Mach-number independent [7]. Integral parameters, such as the coefficient of drag, have been shown to be only mildly affected by Mach number in the hypersonic flow regime [19]. Since the location of separation has little effect on these parameters, the specific problem of laminar separation in the wake has received less attention.

Two dimensional simulations of the compressible Navier-Stokes equations were performed using an open-source CFD software, OpenFOAM, to quantify the relationship between separation location, Mach number and Reynolds number for a circular cylinder in supersonic flows. Simulations were performed over a range of Mach ($2 < Ma < 10$) and Reynolds ($10^3 < Re < 10^5$) numbers. As well, a series of simulations were performed with the no-slip condition removed at the wall. These simulations were used to quantify the effect of Mach number on the flow-field without the presence of a boundary layer. The viscous simulation results were validated against experimental data. The results were also compared to an empirical correlation formulated by Park *et al.* (2010). The formulated empirical relation assumed Mach number independence and that the surface pressure minimum was an acceptable approximation of the separation location [7]. The validity of both assumptions is unknown. It is proposed here that a significant component of the experimental scatter that is observed is related to a Reynolds/Mach number dependence and a significant difference between the location of the surface pressure minimum and the actual separation point at some of the conditions. The extent that the empirical correlation can be used to accurately predict separation is a motivation for this work.

2 Theoretical Background

In the present discussion of the near-wake separated region, a similar analogy to that used by Grange, Klineberg and Lees [11,16] is used to directly compare the laminar near wake, to the separated region occurring in similar flows [20]. In particular, the flow in a compression corner has similar features. In both cases, an adverse pressure gradient due to the presence of a shock-wave causes the boundary layer to separate, and reattach downstream. This creates a region of recirculating flow, including a stable supersonic free-shear layer. As well, the requirement for the presence of a shock is created because of an instantaneous change of flow direction in the two cases. In the case of a compression corner, the shock forms because the flow is redirected by the wall. Similarly in the case of a cylinder, the shock forms because the flow is redirected downstream from the symmetry condition at the centerline. In both cases, a weaker separation shock forms at the beginning of the interaction region, followed by a reattachment (or recompression) shock. In the compression corner, the reattachment shock redirects the flow to be tangential to the wall, and on the cylinder the flow is redirected to be aligned with the centerline. Figures 1 and 2 compare the flow topology between the two cases.

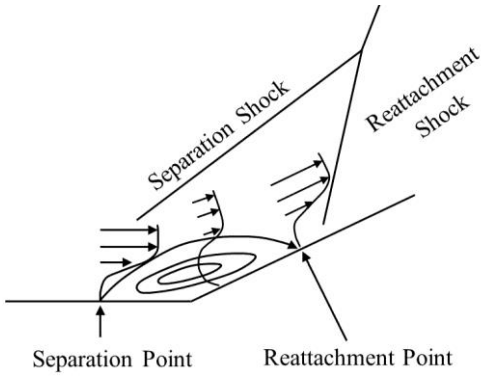

Fig. 1 - Flow Topology: Compression Corner

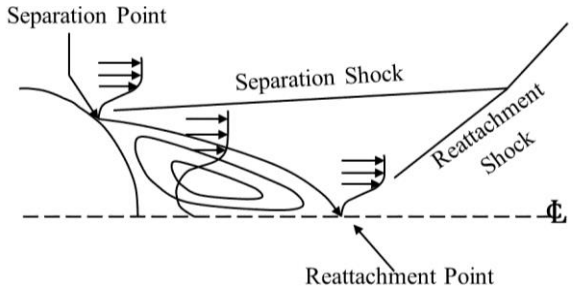

Fig. 2 - Flow Topology: Cylinder Near-Wake

Babinsky and Harvey [21] use the boundary layer shock pressure jump competition concept to explain how momentum and shear forces compete against an adverse pressure gradient to withstand separation. Equation 1 gives the non-dimensional compressible conservation of momentum equation in the x-direction. The magnitude of the shear term is inversely proportional to Reynolds number. In general, the derivative of the shear force in the surface normal direction $\partial\tau/\partial y$ is negative and both adverse pressure and shear stress work to retard the flow momentum. However in the region of interaction between the adverse pressure gradient and the boundary layer, $\partial\tau/\partial y$ becomes positive and thus competes against the pressure gradient that is causing the flow to separate.

$$\frac{\partial \rho^* u^*}{\partial t^*} + \frac{\partial \rho^* u^{*2}}{\partial x^*} + \frac{\partial \rho^* u^* v^*}{\partial y^*} = -\frac{\partial p^*}{\partial x^*} + \frac{1}{Re}\left[\frac{\partial \tau^*_{xx}}{\partial x^*} + \frac{\partial \tau^*_{xy}}{\partial y^*}\right] \quad (1)$$

When the boundary layer is approaching separation, as the local surface Reynolds number is increased, the relative magnitude of shear forces in the boundary layer decrease (see Eq. 1), and the boundary layer becomes more sensitive to separation from the adverse pressure gradient [21]. Based on these analogies, it is to be expected that an increase in Reynolds number would result in a decrease of separation length (the distance between the pressure minima and the point of separation).

It is known from past experiments and investigations [8,11-16] that both the pressure minima and the separation point are affected by Reynolds number. The pressure minima by definition coincides with the beginning of the onset of adverse pressure in the boundary layer. This dependence on Reynolds number indicates an intrinsic relationship between boundary layer displacement effects and the formation and location of the lip separation shock.

2 Simulation Set-up

2.1 Thermodynamics and Viscosity Modelling

Characterizing hypersonic flow using similarity parameters such as Mach number and Reynolds number is inherently limited by the dependence on temperature dependent gas properties. Thus, the specific and quantitative conclusions drawn are gas specific, however general qualitative relationships between parameters should still hold for different gases. To ensure realistic results, the gas selected for the simulation was Nitrogen because of its similarity to air, and its low levels of dissociation below Mach 10.

To model the temperature dependence of gas thermodynamic properties, a 7-coefficeint NASA thermodynamics relation, based on the NIST-JANAF thermochemical tables [22], was used for Nitrogen. The JANAF thermodynamics model accounts for the changes to the enthalpy of the gas, as long as the gas remains in thermal equilibrium. The polynomial coefficients utilized are valid from 100 K to 6000 K.

Sutherland's law was used to model the viscosity. The form of Sutherland's law used is valid up to approximately 3000K [23].

2.2 Solver

The open source computational fluid dynamics (CFD) software, OpenFOAM v.2.2.1, with the solver, rhoCentralFoam, was used to simulate the problem. The flow is assumed to be laminar, in equilibrium, and a continuum. The gas is treated as an ideal gas. The solver rhoCentralFoam is a density based central difference solver of the unsteady, compressible Navier-Stokes equations [24]. The central discretization scheme used by rhoCentralFoam makes it less susceptible to spurious numerical oscillations at strong flow discontinuities such as shockwaves [24,25]. This makes rhoCentralFoam an appropriate solver in the present case because of the strong bow shock and density gradients present in the flow.

2.3 Geometry and Boundary Conditions

The inlet boundary condition was given a fixed velocity, pressure and temperature for each simulation. The inlet temperature for all conditions was 158 K. The Reynolds number and Mach number were manipulated with velocity, and pressure, and calculated assuming an ideal gas, and Sutherland's viscosity law. In the slip cases, the wall of the cylinder was given a slip boundary condition. In the fully viscous case, the boundary was treated as no slip. In both cases, the surface of the cylinder was treated as adiabatic (zero-gradient temperature). The far-field boundaries (the top, bottom, and exit) of the domain were given zero gradient boundary conditions. The simulation domain was sized to provide adequate distance to allow near wake development with no boundary condition interference, while minimizing the computational time. Unlike subsonic flow cases, where the domain edges must be placed far away from any important flow feature, in the supersonic case, the domain need only be sized to ensure that boundary is entirely supersonic [19]. The domain was sized with 10 radii in the downstream and perpendicular directions, and 5 radii in the upstream direction.

The simulation mesh was generated using a block grid created in the native OpenFOAM meshing utility blockMesh. Due to the wide range of simulation conditions, to minimize total simulation time, a mesh independent working grid of 400 000 hexahedral elements was used. Mesh independence was performed on a grid of approximately 920 000 elements. A maximum deviation between coarse and refined grid of < 3% was achieved for separation location, and pressure distribution.

3 Assumptions

The flow was assumed to be laminar and in chemical and thermal equilibrium. The simulation results were analyzed to assess the validity of these assumptions.

3.1 Turbulence

There are two main instability modes that cause transition in supersonic flows. The first, which is dominant in subsonic flows, involves the growth of local disturbances, leading to the spreading of turbulent spots, and eventually full turbulence [26]. It was shown by both Fiala *et al.* (2006), and Krishnan *et al* (2006) that increasing the freestream Mach number over a flat plate corresponds to a decrease the spreading rate of turbulent spots, delaying transition, up until approximately Mach 4 [26,27]. Above Mach 4, the inviscid Mack mode instability becomes important while the first mode becomes further suppressed [28,29]. While there is a general understanding of the cause and effect relationship of various supersonic flow parameters (Re, Ma) on transition, a complete model of transition does not exist. Eli Reshotko explained that obtaining a simplified general transition model for these conditions is an unrealistic expectation [30]. However, several transition criteria exist and these were utilized to investigate the validity of the assumption of 2D laminar flow. A transition criterion commonly used for reentry-type geometries, such as the MSL aeroshell, is the local momentum thickness Reynolds number (Re_θ = 200) [31]. However, it has been established that transition on circular cylinders at supersonic speeds generally occurs in the wake before it occurs on the body [32]. A near-wake transition criteria ($Re_{fs} < 5.6x10^4$) was given by Lees (1964) based on a Reynolds number that uses wake edge properties and the length of the free-shear layer as the characteristic length scale. Both of these criteria were analyzed closely for high Reynolds number simulations. Simulations that did not satisfy these criteria were not included in any subsequent analysis.

3.2 Chemical and Thermal Equilibrium

The simulation results were also analyzed to determine if chemical or thermal non-equilibrium effects are significant for any of the operating conditions. The dissociation of diatomic molecules (such as Nitrogen gas), occurs approximately between 3000 and 7000 K [33]. The highest post-shock equilibrium temperature simulated, corresponding to the Mach 10 condition, was approximately 2900 K. An equilibrium calculation of Nitrogen, using a

STANJAN chemical equilibrium calculator [34], was performed at this temperature (≈2900 K) and at the lowest post shock stagnation pressure (≈1700 Pa). The results showed a mass fraction of $2.7x10^{-5}$ of dissociated Nitrogen at this condition, indicating that dissociation effects are negligible.

Only vibrational non-equilibrium was considered as a potential non-equilibrium effect. Rotational and translational temperatures reach equilibrium after a few molecular collisions, which is equivalent to a convective distance of the shock wave thickness [33]. In contrast, several thousands of collisions are required for the vibrational temperature to reach equilibrium, resulting in a vibrationally thick shock wave [33]. The worst case for thermal non-equilibrium effects are low Reynolds number, high Mach number combinations because of larger temperature changes, and longer vibrational relaxation times. In the worst case examined (Ma=10, Re=2500) the maximum estimated error in temperature was < 18% downstream of the shock. The results of the simulations where the potential error due to non-equilibrium is suspected are still included because the effects of non-equilibrium are not a focus of the present study. There is still value in the inclusion of these results, because the objective of this work is to establish the relationship between Mach number, Reynolds number and the near wake under the assumption of equilibrium, which in general, should not be gas specific. Whereas, the state of non-equilibrium is gas specific.

4 Results and Discussion

4.1 Slip Simulation Results

To demonstrate the effect of Mach number on flow separation, and the flow in general, simplified simulations were performed with the no slip condition removed from the boundary conditions at the wall. While viscous effects still exist in the outer flow, this removes the importance of any Reynolds number defined based on the cylinder length scale. There is no boundary layer development on the body and any viscous stresses in the flow field must be generated by gas dynamic effects.

Figure 3 shows stream lines in the near wake of the flow at a representative Mach number; Mach 8. Similar results in flow structure were present at all Mach numbers simulated. The recirculation zone in the near-wake is clearly seen. It is obvious that the reversal of the flow in the near wake does not hinge on the presence of a boundary layer on the body and is a result of the lip separation shock and gas dynamic effects primarily.

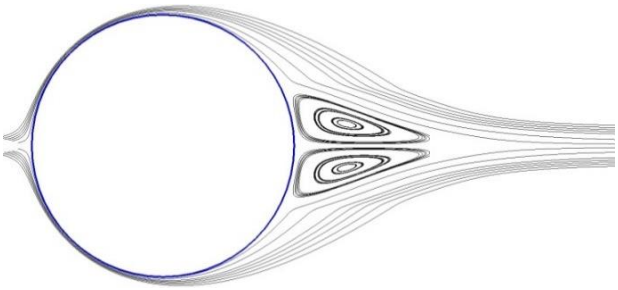

Fig. 3 - Slip Simulation Results (Mach 8)

The recirculation zone formed in the slip simulations is a result of the shock that must be formed in order to suddenly direct the flow to the center-line (similar to the situation in a compression corner or forward facing step). The formation and size of the recirculation zone is due to this deflection. Since the flow-field is viscous, the deflected flow entrains fluid from the subsonic “dead air” region via viscous shear. As the two deflected streams come together in the neck region of the wake, a situation of mass imbalance occurs, and some flow must be redirected back toward the cylinder in order to constantly feed the flow entrained in the shear layer. This concept is usually explained using the concept of the dividing streamline [7,11,16,20,21].

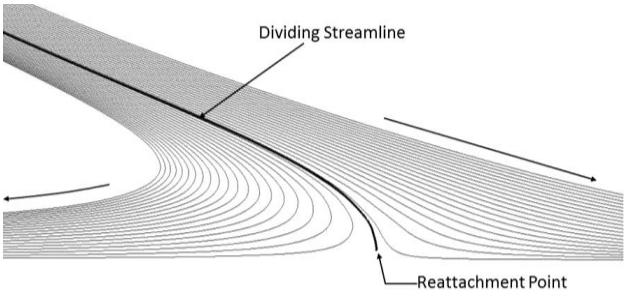

Fig. 4 - Streamlines in Reattachment Region

Figure 4 shows the streamlines, including the dividing streamline, in the reattachment region. All of the streamlines above the dividing streamline continue past reattachment, and all of those below it are redirected back towards the body.

The Mach number effect on the location of the aft-body shock in the slip simulations was also observed. The strength and location of impingement of the shock wave in a shock-wave boundary layer interaction is a fundamental parameter as it acts as a forcing function that dictates the adverse pressure gradient, the upstream influence of the interaction, and the separation location [20,21]. The observations in the slip simulation lead to helpful conclusions in describing the effect of Mach number on the location and strength of the lip separation shock in the viscous simulations. Figure 5 shows the resulting static pressure distribution on the leeward surface of the circular cylinder at various free-stream Mach numbers with the no-slip condition removed at the wall.

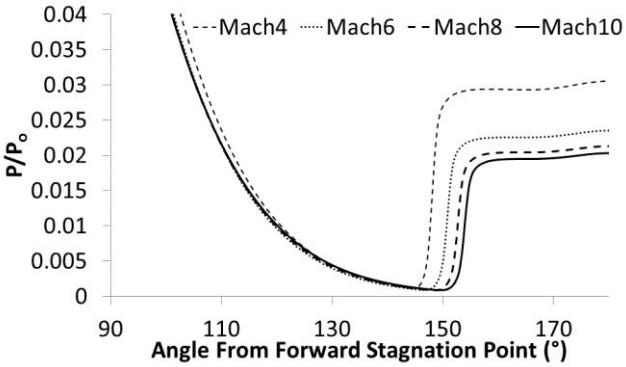

Fig. 5 - P/P_o vs. Angle from Forward Stagnation Point

The results of the simulations show that as the free stream Mach number is increased, the angle at which the lip separation shock forms (and the angle where the flow reverses) increases, and the strength of the lip separation shock decreases. An asymptotic relationship, concurrent to the expected trend of hypersonic Mach number independence, is observed between lip separation shock strength and location as Mach number increases. The convergence is observed since the strength and location of the shock-wave are quantitatively close (< 5%) between Mach 8 and Mach 10.

4.3 Viscous Simulation Results

Fully viscous simulations were simulated to examine the combined effects of Mach and Reynolds Numbers. Figure 6 shows a synthetic schlieren image of a simulation at Mach 10 and a free-stream Reynolds number ~5.5×10^4. The figure shows clearly the flow structures that are explained in detail in the literature [7,11,12,14].

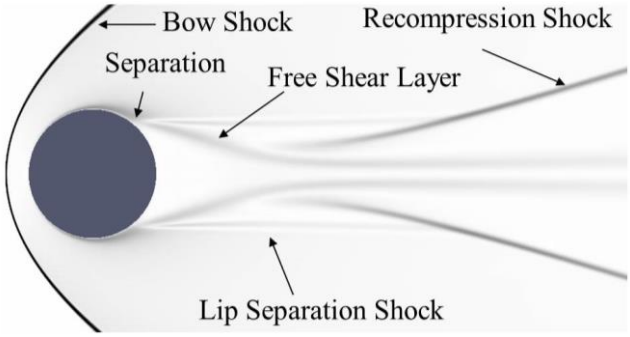

Fig. 6 - Typical Hypersonic Cylinder Flow Topology (Ma=10; Re≈5.5×10^4)

4.3.1 Comparison to Experiment

The results of the present simulation were compared to the experiments completed by McCarthy and Kubota [14]. Figure 7 shows a comparison of the pressure distribution in the base region from one of the experiments completed by McCarthy *et al.* (1956). The pressure distribution is known to be a net result of viscous-inviscid interaction between the boundary layer development and the free stream gas dynamics, and thus a consequence of the physics attempted to be modelled in the simulation. The results of the simulation show good agreement with the experimental results. The predicted pressure distribution lies within, or just outside of the reported error of the experiment. This closeness was present with the other experiments performed by McCarthy as well. Some error is present because the free-stream Mach and Reynolds numbers reported by McCarthy are approximate or nominal values, and thus may not exactly match the simulated values. As well, the McCarthy experiments were done with air as the free-stream test gas, while the present simulations are simulated

utilizing Nitrogen (see Section 2). However, at Mach 6, the thermal and transport properties of Nitrogen and Air are expected to be similar and thus the close agreement is expected.

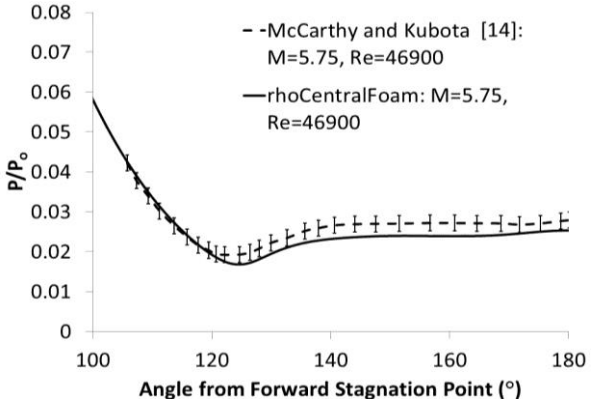

Fig. 7 - Comparison to Experimental Measurements of McCarthy and Kubota [14]

4.3.2 Reynolds Number Dependence

It is established that Reynolds number has a significant effect on separation, particularly in laminar boundary layer flows [8,7,11,21]. Figure 8 shows the results for the separation point (location of zero wall shear stress), and the pressure minimum location as a function of free stream Reynolds number at a free-stream Mach number of 5.86. The results shown in Figure 8 show that both the pressure minima location and the separation point are a function of Reynold's number. As well, the distance between the separation point and pressure minima, known as the separation length, decreases as Reynolds number is increased. Separation length is plotted in Figure 9 vs. free-stream Reynolds Number. The maximum coefficient of friction (Equation 7) vs. free-stream Reynolds number is shown in Figure 10.

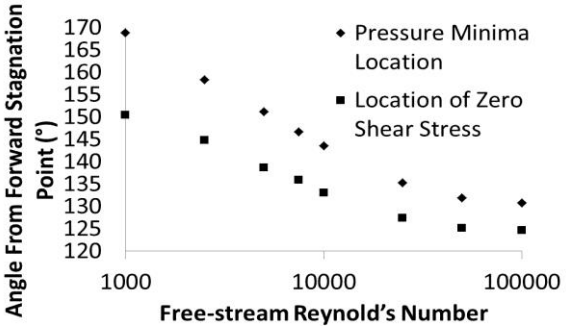

Fig. 8 - Location of Pressure Minima and Zero Shear-stress Location vs. Free-stream Reynolds Number

These results confirm the relationship described in Section 2 regarding the competition between shear stress and stream-wise adverse pressure. As Reynolds number is increased, the magnitude of the viscous stress decreases, and the boundary layer becomes more sensitive to the adverse pressure gradient.

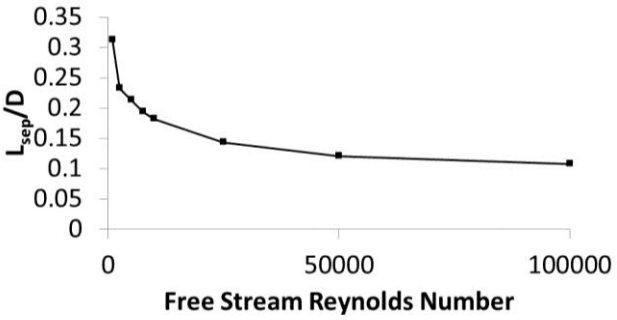

Fig. 9 - Separation Length vs. Free-Stream Reynolds Number (Mach 5.86)

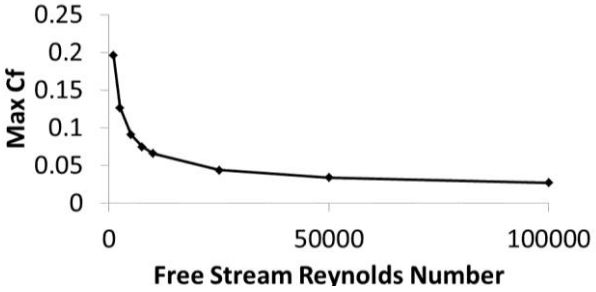

Fig. 10 - Maximum C_f vs. Free Stream Reynolds Number (Mach 5.86)

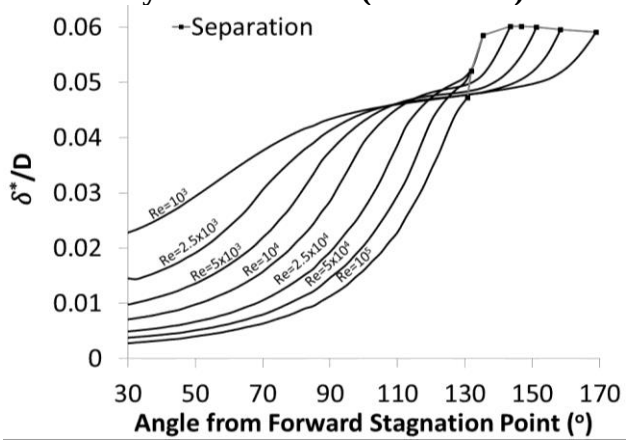

Fig. 11 - δ*/D vs. Angle from Forward Stagnation Point (Mach 5.86)

As explained in Section 2, the dependence of the pressure minima location on Reynolds number should be able to be explained by examining the inviscid-viscous interaction between the boundary layer and the free-stream. The boundary layer acts to displace the free-stream and alter the effective shape of the

cylinder, and thus the pressure distribution. In Figure 11, the displacement thickness as a function of the angle from the forward stagnation point is plotted at various Reynolds numbers.

As the Reynolds number changes, the development of the boundary layer (the profile of displacement thickness on the body) changes. At low Reynolds numbers, the displacement thickness (δ^*) of the boundary layer is large, and prevents separation until a high angle on the cylinder surface. At these low Reynolds numbers, no lip separation shock occurs. The boundary layer results in a gradual compression of flow leading to a more modest pressure gradient. As the Reynolds number is increased, this effect decreases and the gradual compression of the free-stream eventually at higher Reynolds numbers becomes the lip separation shock wave. As the effect of the boundary layer on the free-stream decreases, the mitigating effect of the boundary layer on the radius of curvature of the body declines. This causes the lip separation shock to form earlier and results in moving the pressure minima and the separation point upstream.

4.3.3 Mach Number Dependence

The results show that the principal of hypersonic Mach number independence is not an accurate assumption regarding separation location. Even at high Mach numbers, the effect is in fact not negligible, but is directly interconnected with Reynolds number. Figure 12 shows the separation angle vs. Mach number at two representative Reynolds numbers.

From Figure 12 it is observed that the rate at which the location of separation approaches Mach number independence is affected heavily by Reynolds number. At a Reynolds number of 10^5, the flow separation location is less dependent on Mach number. However, at smaller Reynolds numbers (eg. $Re=10^4$) the angle of separation is highly dependent on Mach number. This type of relationship is to be expected since as $Re\rightarrow\infty$ the Navier-Stokes equations become the Euler equations from which hypersonic Mach number independence is derived.

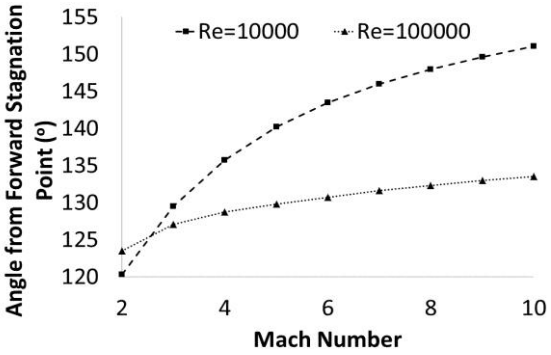

Fig. 12 – Effect of Mach Number on Separation Angle

As well, at high Reynolds numbers, the magnitude of viscous forces is greatly reduced, and thus the viscous-inviscid interaction due to boundary layer development decreases in importance, and the effect of Mach number is greater. Figure 13 shows the effect of Mach number on boundary layer displacement thickness development.

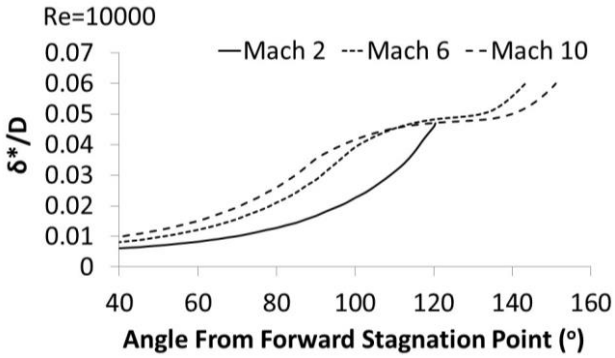

Fig. 13 – δ*/D vs. Angle from Forward Stagnation Point (^{o})

4.3.4 Comparison to Empirical Formula

In the past, the location of the surface pressure minima has sometimes been treated as an adequate approximation of the location of separation because of the close proximity between the two [7]. However, at lower Reynolds numbers, the difference between the pressure minima location and the true point of separation can be larger. In the research presented by Park *et al.* (2010), pressure data was collected from a wide range of experiments, ranging in both Mach number and Reynolds number [7]. The pressure minimum location was extracted from the data, and an empirical relation was given for separation location, based on the assumption that this minimum was the

location of separation, and that Mach number effects were negligible. The Mach numbers in the experiments examined ranged from M=2 to M=14.97. The Mach numbers in the experiments examined in the study that corresponded to cylinders with nearly adiabatic walls ranged from M=2 to M=6. The resulting empirical relation is shown in Equation 8.

$$\theta_{separation} = 116.3 + 577 Re_{\mu}^{-0.5} \qquad (8)$$

Figure 14 shows the location of pressure minima and the true separation location at various Mach numbers (Ma=2 to Ma=6), and for various Reynolds numbers plotted as $Re_{\mu}^{-0.5}$, to match the independent variable of Equation 8. This Reynolds number is defined using the post shock viscosity.

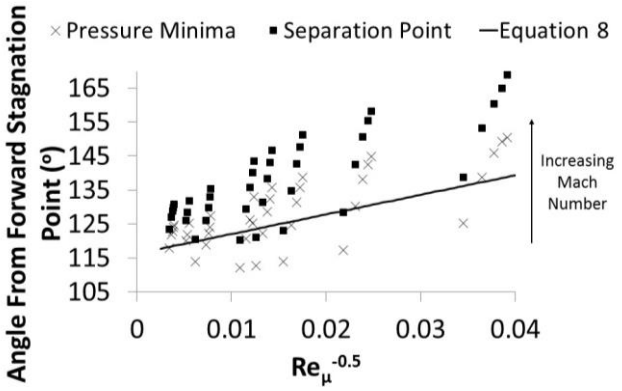

Fig. 14 - Comparison of Separation angle, Pressure Minima Angle and Equation 8

Equation 8 shows qualitative agreement with the simulation results for pressure minima location. The maximum error between the simulation results and empirical relation is ~12%. However, when compared to the location of separation based on the wall shear stress, the error is larger (~20%). The discrepancy between the predicted pressure minima location is likely due to the fact that Mach number is neglected in Equation 8.

5 Conclusion

Simulations were performed over a wide range of Mach numbers, and Reynolds numbers to demonstrate the effect of these changing parameters on the near wake separation on the aft-body of circular cylinders. Simulations were validated through comparison against experimental results. Simulation results were used to closely examine the physics of separation, and the shock-wave boundary layer interaction that occurs. It was shown through the parametric study, that the commonly held principal of hypersonic Mach number independence is not applicable to near-wake separation. The results indicate a highly interdependent relationship between Mach number and Reynolds number due to boundary layer displacement effects on the free-stream, and the effect of viscous shear on the resilience of boundary layers to adverse pressure. The proximity of the pressure minima to the point of separation agreed well with accepted theory of shock-wave boundary layer interactions in that it was found to be closely dependent on Reynolds number.

Acknowledgements

This research was enabled in part by support provided by WestGrid (www.westgrid.ca) and Compute Canada Calcul Canada (www.computecanada.ca).

References

[1] Lykoudis, P. S., A Review of Hypersonic Wake Studies, Memo RM 4493, Advanced Research Projects Agency, Rand Corp., May 1965.

[2] Button, E.C, Lilley, C. R., Mackenzie, N.S., Sader, J.E., Blunted-Cone Heat Shields of Atmospheric Entry Vehicles, *AIAA Journal*, Vol. 47, No. 7, pp. 1784-1787, 2009.

[3] Schneider, S. P., Effects of Roughness on Hypersonic Boundary-Layer Transition, *Journal of Spacecraft and Rockets*, Vol. 45, No. 2, pp. 193-209, 2008.

[4] Johansen, C., Novak, L., Bathel, B., Ashcraft, S., and Danehy, P. Mars Science Laboratory Reaction Control System Jet Computations with Visualization and Velocimetry, *Journal of Spacecraft and Rockets*, Vol. 50, No. 6, pp. 1183-1195, 2013.

[5] A.A. Dyakonov, M. Schoenenberger, W.I., Scallion, J.W. Van Norman, L.A. Novak, C.Y. Tang, Aerodynamic interference due to MSL Reaction Control System, AIAA Paper 2009-3915, *41st AIAA Thermophysics Conference*, San Antonio, TX, 2009.

[6] Johansen, C., Danehy, P., Ashcraft, A., Bathel, B., Inman, A., Jones, S., Planar Laser-Induced Fluorescence of Mars Science Laboratory Reaction Control System Jets, Journal of Spacecraft and Rockets, Vol. 50, pp. 781-792, 2013.

[7] Park, G., Gai, S. L., Neely, A. J., Laminar Near Wake of a Circular Cylinder at Hypersonic Speeds, *AIAA Journal*, Vol. 48, No. 1, pp. 236-247, 2010.

[8] Weiss, R., Base Pressure of Slender Bodies in Laminar, Hypersonic Flow, *AIAA Journal*, Vol. 4, No. 9, pp. 1557-1559, 1966.

[9] Denison, M. R., Baum, E., Compressible Free Shear Layer with Finite Initial Thickness, *AIAA Journal*, Vol. 1, No. 2, pp. 342-349, 1963.

[10] Baum, E., King, H. H., Denison, M. R., Recent Studies of the Laminar Base-Flow Region, *AIAA Journal*, Vol. 2, No. 9, pp. 1527-1534, 1964.

[11] Grange, J., Klineberg, J. M., Lees, L., Laminar Boundary-Layer Separation and Near-Wake Flow for a Smooth Blunt Body at Supersonic and Hypersonic Speeds, *AIAA Journal*, Vol. 6, No. 6, pp. 1089-1096, 1967.

[12] Dewey, C. F. Jr., Near Wake of a Blunt Body at Hypersonic Speeds, *AIAA Journal*, Vol. 2, No. 6, pp. 1001-1010, 1965.

[13] Chapman, D. R., Investigation of Separated Flows in Supersonic and Subsonic Streams with Emphasis on the Effect of Transition, NACA Rept., No. 1356, pp. 421-460, 1957.

[14] McCarthy, J. F., Kubota, T., A study of wakes behind a cylinder at M equal 5.7, *AIAA Journal*, Vol. 2, No. 4, pp. 629-636, 1964.

[15] Tewfik., O. K., Heat Transfer Recovery Factor, and Pressure Distributions Around a Circular Cylinder, Normal to Supersonic Rarefied-Air Stream, *Journal of the Aerospace Science*, Vol. 27, No. 10, pp. 721-729, 1960.

[16] Reeves, B., Lees L., Theory of Laminar Near Wake of Blunt Bodies in Hypersonic Flow, *AIAA Journal*, Vol. 3, No. 11, pp. 2061-2074, 1965.

[17] Bashkin, V. A., Vaganov, A. V., Egorov, I. V., Ivanov, D. V., Ignatova, G. A., Comparison of Calculated and Experimental Data on Supersonic Flow Past a Circular Cylinder, *Fluid Dynamics*, Vol. 37, No. 3, pp. 473-483, 2002.

[18] Gregorek, G. M., Korkan, K. D., An experimental observation of the Mach and Reynolds-Number Independence of Cylinders in Hypersonic Flow, *AIAA Journal*, Vol. 1, No. 1, pp. 210-211, 1962.

[19] Anderson, J. D., *Modern Compressible Flow with Historical Perspective*, Hypersonic Flow, 3rd ed., Vol. 1, McGraw-Hill, New York, pp. 565-569, 2003.

[20] Lees, L., Reeves, B., Supersonic Separated and Reattaching Laminar Flows: I. General Theory and Application to Adiabatic Boundary-layer/Shock-wave Interactions, *AIAA Journal*, Vol. 2, No. 11, pp. 1907-1920, 1964.

[21] Babinsky, H., Harvey, J. K., *Shock Wave-Boundary-Layer Interactions*, 1st Edition, Cambridge University Press, 2011.

[22] NIST-JANAF (2013), *NIST-JANAF Thermochemical Tables*, Retrieved February 2014, from http://kinetics.nist.gov/janaf/

[23] Rathakrishnan, E. *Theoretical Aerodynamics* Properties of Fluids, 1st ed., Vol.1, John Wiley & Sons Singapore, pp. 23-28, 2013.

[24] Greenshields, G. J., Weller, H. G., Gasparini, L., Reese, J. M., Implementation of semi-discrete, non-staggered central schemes in a collocated, polyhedral, finite volume framework, for high-speed viscous flows, *International Journal for Numerical Methods in Fluids*, 2009

[25] Arisman, C. J., Johansen, C. T., Galuppo, W. C., McPhail, A., Nitric Oxide Chemistry Effects in Hypersonic Boundary Layers, *43rd AIAA Fluid Dynamics Conference*, 2013.

[26] Fiala, A., Hillier, R., Mallinson, S. G., and Wijesinghe H.S., Heat Transfer Measurement of turbulent spots in a hypersonic blunt-body boundary layer, *Journal of Fluid Mechanics*, Vol. 555, pp. 81-111, 2006.

[27] Krishnan L., and Sandham, N. S., Effect of Mach Number on the Structure of Turbulent Spots, *Journal of Fluid Mechanics*, Vol. 555, pp. 225-234, 2006.

[28] Mack, L. M., Transition Prediction and linear stability theory, Agard CP 224, NATO, PARIS

[29] Larson, H. K., Keating, S. J. Jr., Transition Reynolds numbers of separated flows at supersonic speeds, NASA TN D-43, 1960

[30] Reshotko, E., Transition Prediction: Supersonic and Hypersonic Flows, NATA-OTAN, RTO-EN-AVT-151

[31] Hollis, B. R., Blunt-Body Entry Vehicle Aerothermodynamics: Transition and Turbulent Heating, *Journal of Spacecraft and Rockets* , Vol. 49, No. 3, pp. 435-449, 2012.

[32] Lees, L., Hypersonic Wakes and Trails, *AIAA Journal*, Vol. 6, No. 6, pp. 417-428, 1964

[33] Zel'dovich, Y. B., Physics of Shock waves and high temperature hydrodynamic phenomena, USAF Translation

[34] Dandy, D. (2014), *Chemical Equilibrium Calculator*, Retrieved February 2014, from http://navier.engr.colostate.edu/~dandy/code/code-4/

[35] ICAS (2014), ICAS 2014 Report Template, Retrieved July 9, 2014, from http://www.icas.org/

Copyright Statement